Electronic Supplementary Information for:

Hydrogen bond-rigidified planar squaraine dye and its electronic and organic semiconductor properties

Takeshi Maeda,[a]* Andreas Liess,[b] Astrid Kudzus,[b] Ana-Maria Krause,[b] Matthias Stolte,[b] Hitoshi Amitani,[a] Shigeyuki Yagi,[a] Hideki Fujiwara[c] and Frank Würthner[b]*

[a]Graduate School of Engineering, Osaka Prefecture University, Sakai 599-8531, Japan.
E-mail: tmaeda@chem.osakafu-u.ac.jp
[b]Institut für Organische Chemie and Center for Nanosystems Chemistry, Universität Würzburg, Am Hubland, 97074 Würzburg, Germany.
E-mail: wuerthner@uni-wuerzburg.de
[c]Graduate School of Science, Osaka Prefecture University, Sakai 599-8531, Japan.

Table of Contents

1. Materials and methods

NMR spectra were obtained using JEOL ECX-400 or ECS-400 spectrometers operating at 400 MHz for ^{1}H-NMR and 100 MHz for ^{13}C-NMR. Chemical shifts were reported in parts per million (δ) downfield from tetramethylsilane (TMS) as an internal standard in $CDCl_3$. FT-IR spectra were recorded using a Shimadzu FT-IR 8400S spectrophotometer. The electrospray ionization mass spectra (ESI-MS) were recorded on a JEOL JMS-T100CS spectrometer using methanol-dichloromethane (1/1, v/v) as eluents. The elemental analyses were performed on a Yanako CHN CORDER JM-10 analyzer. The absorption spectra were measured in a 1.0 cm quartz cell on a Shimadzu UV-3600 spectrophotometer. The fluorescence spectra were recorded on a JASCO FP-6600 spectrofluorometer using a 1.0 cm quartz cell. Fluorescence lifetimes were measured using a Horiba Jobin Yvon FluoroCube spectroanalyzer with a 567 nm LED light source for excitation. A colloidal silica suspension in water was used as scatterer to determine the instrumental response. Fluorescence quantum yields were measured in THF at 25ºC using a Hamamatsu Photonics C9920 PL quantum yield measurement system. The oxidation potential of the dye was measured on Hokuto Denko HZ-5000 electrochemical measurement system at a scanning rate of 100 mV s^{-1}, equipped with a normal one-compartment cell with a glassy carbon working electrode, a Pt counter electrode, and a nonaqueous $Ag/AgNO_3$ reference electrode. The measurement was performed in a dichloromethane solution including 0.1 M tetrabutylammonium hexafluorophosphate as a supporting electrolyte. The thermogravimetric analyses were performed on RIGAKU Thermoplus EVO TG-DTA at the heating rate of 10 °C/min^{-1}. All solvents and reagents were purchased from commercial sources and used as received without further purification. Silica gel (SiO_2, spherically-shaped, neutral) for the flash chromatography was purchased from Kanto chemical (Tokyo, Japan). Spectroscopic-grade solvents were purchased from Wako Pure Chemicals (Osaka, Japan) and used immediately after opening for all spectroscopic measurements. 2,3,3-trimethyl-3*H*-indolenine (**3a**) were purchased from Tokyo Chemical Industry (Tokyo, Japan). 5-fluoro-2,3,3-trimethyl--3*H*-indolenine (**3b**) and triethylammonium 2-ethoxy-3-dicyanomethylidene-4-oxocyclobut-1-en-1-olate (**4**) were prepared according to the literature.[1-3]

2. Film and OTFT fabrication and characterization

Fabrication: 30 nm thin squaraine films were vacuum-deposited onto *n*-tetradecylphosphonic acid (TPA, Alfa Aesar) modified Si/SiO_2 (100 nm)/AlO_x (8 nm, grown by atomic layer deposition) substrates (1.7 nm TPA monolayer; capacitance $C_i = 32.4$ nF cm^{-2}) with the evaporation system OPTIvap-XL (Creaphys GmbH). The TPA-modified substrates are a kind donation of Dr. Hagen Klauk and Dr. Ute Zschieschang (MPI für Festkörperforschung, Stuttgart). During the deposition of the squaraine dyes, a growth rate of 0.2-0.6 nm min^{-1} was adjusted by monitoring the film growth with a quartz crystal microbalance and the pressure was below 10^{-6} mbar. Furthermore, the substrate temperature (T_S) was kept constant at a fixed temperature of 60 °C or 80 °C for **1H** or 100 °C for **1F**. Subsequently, 30 nm gold were evaporated through steel shadow masks onto the films to form the source and drain electrodes, finally yielding devices with a channel length L and width W of 100 and 200 μm, respectively. *Characterizations*: The transistor current voltage characteristics were measured under inert conditions (MBraun Intergas System GmbH, UNIlab Pro, $c(O_2) < 1$ ppm, $c(H_2O) < 1$ ppm) using an Agilent 4155C semiconductor parametric analyzer (Agilent Technologies, Inc., Santa Clara, CA) with a Cascade EPS150 probe station. For the OTFT devices, the semiconducting film around the device was scratched with a needle of the used Micromanipulator to electrically isolate the device prior to characterization. Atomic force microscopy was done with a Bruker AXS MultiMode™ Nanoscope IV instrument in the tapping mode. Silicon cantilevers (OMCL-AC160TS, Olympus) with a spring constant of 42 N m^{-1} and a resonance frequency of ~300 kHz were used. UV-Vis measurements of thin films on Si/Al/AlO_x/TPA substrates were performed in reflection mode using an OceanOptics Maya2000 Pro spectrometer.

3. Synthesis and characterization of squaraine dyes

*Synthesis of **1H*** 2,3,3-trimethylindolenine (**3a**) (199 mg, 1.25 mmol) and triethylammonium 2-ethoxy-3-dicyanomethylidene-4-oxocyclobut-1-en-1-olate (**4**) (200 mg, 0.626 mmol) were dissolved in a mixture of 1-butanol/benzene (1/1, 6 mL). A drop of conc. H_2SO_4 was added, and then the solution was heated under reflux overnight. After cooling, the solvent was removed on a rotary evaporator, and the residue was purified by silica gel column chromatography (eluent: $CHCl_3$) and the first green band was collected. After the solvent was removed at reduced pressure, the residue was dissolved in the minimal amount of chloroform and precipitated from hexane to obtain the product as a reddish brown solid (118 mg, 0.423 mmol, 68%). ^{1}H NMR ($CDCl_3$, 400 Mz): δ 12.3 (s, 2H), 7.36-7.30 (m, 4H), 7.23-7.21 (d, 2H, J = 7.8 Hz), 7.18-7.14 (m, 2H), 5.81 (s, 2H), 1.47 (s, 12H). ^{13}C NMR ($CDCl_3$, 100 MHz): δ 178.50, 176.76, 162.90, 162.47, 141.26, 139.37, 129.79, 128.50, 124.30, 122.74, 116.96, 111.90, 87.10, 49.63, 26.41. IR (neat film, cm^{-1}): 2197, 1618, 1551, 1487, 1462, 1340, 1304, 1292, 1188, 1163, 1122, 1111, 1082. 947, 860, 804, 750, 698, 646. MS (ESI): m/z calcd for $[M(C_{29}H_{24}N_4O)-H]^-$, 443.18; found 443.18. Anal. Calcd for $C_{29}H_{24}N_4O$: C, 78.36; H, 5.44; N, 12.60. Found: C, 78.16; H, 5.32; N, 12.76.

Synthesis of ***1F*** The reaction was conducted according to the same procedure as described for **1H**, using dicyanovinylene-substituted squarate (**4**) (186 mg, 0.582 mmol) and 5-fluoro-2,3,3-trimethyl-3*H*-indole (**3b**) (192 mg, 1.08 mmol) to give product **1F** as a green microcrystalline powder (124 mg, 44 %). ^{1}H NMR ($CDCl_3$, 400 MHz): δ 12.33 (s, 2H), 7.18-7.11 (m, 2H), 7.07-6.98 (m, 4H), 5.79 (s, 2H), 1.48 (s, 12H). ^{13}C NMR ($CDCl_3$, 100 MHz): 178.33, 176.77, 176.75, 162.62, 162.29, 161.48, 159.04, 141.33, 141.25, 137.15, 137.14, 116.71, 115.22, 114.98, 112.40, 112.32, 110.88, 110.63, 87.10, 49.92, 49.89, 46.58, 26.25. IR (KBr, cm^{-1}): 2204, 1604, 1556, 1487, 1479, 1387, 1335, 1302, 1271, 1198, 1178, 1163, 1111, 957, 910, 822, 773. MS (ESI): m/z calcd for $[M(C_{29}H_{22}F_2N_4O) - H]^-$, 479.18; found 479.22. Anal. Calcd for $C_{29}H_{22}F_2N_4O$: C, 72.49; H, 4.62; N, 11.66. Found: C, 72.47; H, 4.74; N, 11.60%.

Synthesis of ***2*** 1-ethyl-2,3,3-trimethylindolenium iodide (0.541 g, 1.72 mmol) and triethylammonium 2-ethoxy-3-dicyanomethylidene-4-oxocyclobut-1-en-1-olate (**4**) (0.200 g, 0.687 mmol) were dissolved in a mixture of 1-butanol (1.5 mL) and benzene (1.5 mL). Then the solution was heated under reflux for 5 h. After cooling, the solvent was removed on a rotary evaporator, and the residue was purified by silica gel column chromatography (eluent: CHCl3), and the product was precipitated from $CHCl_3$–hexane solution to obtain **2** as a green solid (82 mg, 0.164 mmol, 24%). ^{1}H NMR ($CDCl_3$, 400 Mz) : δ 7.41-7.32 (m, 4H), 7.24-7.17 (m, 2H), 7.10-7.03 (m, 2H), 6.51 (s, 2H), 4.14-4.02(q, 4H), 1.78 (s, 12H), 1.47-1.40 (t, 6H). ^{13}C NMR ($CDCl_3$, 100 MHz) : δ (ppm) 173.13, 171.58, 167.86, 166.98, 142.58, 141.59, 128.16, 124.67, 122.45, 119.14, 109.91, 88.89, 49.52, 40.68, 39.35, 26.64, 12.30. IR (KBr, cm^{-1}): 2192, 1718, 1624, 1492, 1481, 1456, 1350, 1286, 1201, 1155, 1109, 1076, 980, 920, 824, 775, 748. MS (ESI): m/z calcd for $[M(C_{33}H_{32}N_4O)]^+$, 500.25; found 500.25. Anal. Calcd for $C_{33}H_{32}N_4O$: C, 79.17; H, 6.44; N, 11.19. Found: C, 79.07; H, 6.44; N, 11.11%.

4. Optimized structures of 1H and 1F obtained by DFT calculation[4]

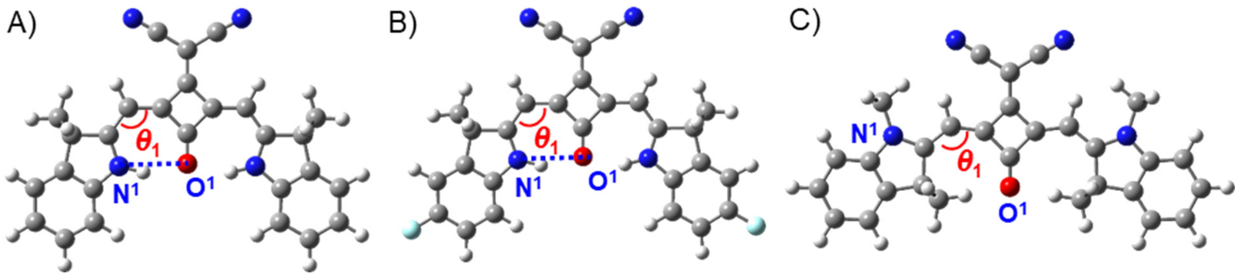

Fig. S1 Optimized Structures of **1H** (A), **1F** (B), and **2** (C) obtained by DFT calculations (B3LYP/6-31+G(d) level).

Table S1. Geometrical parameters (Å and degrees) and values of Mulliken atomic charges calculated at the B3LYP/6-31+G(d) level.

dye	θ_1 (deg)[a]	N^1–O^1 distance (Å)[b]	q_N (a.u.)[c]	q_O (a.u.)[d]
1H	124.7	2.817	−0.361	−0.675
1F	124.6	2.815	−0.365	−0.675
2	133.6	-	−0.092	−0.523

[a] C-C-C bond angles at methine groups. [b]Distances between nitrogen atom of indolenine and oxygen atom of cyclobutenone skeletons. [c]Mulliken charge values at nitrogen atom of indolenines. [d]Mulliken charge values at oxygen atom of cyclobuetnone moiety.

5. Reaction of 2,3,3-trimethylindolenine with squaric acid derivatives

The reactions of *N*-unsubstituted indolenine (Fischer base, **3a**) with parent squaric acid and its butyl ester analogue were conducted under different reaction conditions in order to evaluate the influence of substituents at squaric acid derivatives on the condensation reaction. (Scheme S1, Table S2, Entry 1-5). The condensation of **3a** and squaric acid proceeded in butanol/benzene not only in the presence of basic and acidic additives, but also without any catalyst to give squaraine dye. In cotrast, the reaction of dibutyl squarate with **3a** was observed only under acidic condition. Moreover, the reaction in freshly dried butanol at reflux condition hardly yielded any squaraine product (TableS2, Entry 6-11).

Scheme S1. The reaction of Fischer base and squaric acid derivatives to afford squaraine **5**.

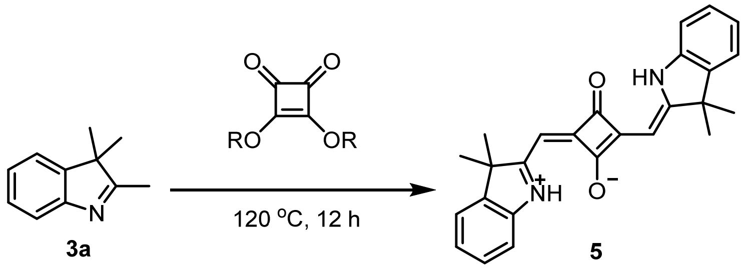

Table S2. The condensation of 2,3,3-trimethylindolenine (**3a**) with squaric acid derivatives (R = H, C_4H_9) under various reaction conditions.[a]

entry	R	solvent, volume ratio	additive	yield (%)[b]
1	H	butanol/benzene, 1/1	non	67
2		butanol/benzene, 1/1	quinoline	43
3		butanol/pyridine, 1/1	non	n. d.
4		butanol/benzene, 2/1	*p*-TsOH	43
5		butanol/benzene, 1/1	H_2SO_4	30
6	C_4H_9	butanol/benzene, 1/1	non	n.d.
7		butanol/benzene, 1/1	quinoline	n.d.
8		butanol/pyridine, 1/1	non	n.d.
9		butanol/benzene, 2/1	*p*-TsOH	21
10		butanol/benzene, 1/1	H_2SO_4	59
11		anhydrous butanol/benzene, 2:1	*p*-TsOH	n.d

[a] The reaction was conducted at azeotropic condition (120 °C) for 12 h. [b] Isolated yield based on **2a**.

Dibutyl squarate can be hydrolyzed under acidic conditions to give the squaric acid monobutyl ester. The hydrolysis product should work as the precursor in the condensation with **3a**.[5] Based on these findings, the reaction condition for condensation of Fischer base **3a** with trimethylammonium 2-ethoxy-3-dicyanomethylidene-4-oxocyclobut-1-en-1-olate (**4**) was studied as shown in Scheme S2 and Table S2. The use of *p*-toluenesulfonic acid as additive promoted the condensation reaction to give *N*-unsubstituted squaraine dye **1H**. The reaction improved significantly by the presence of sulfuric acid to afford the target compound **1H** in 68% yield.

Scheme S2. Synthesis of **1H** from Fischer's base (**3a**) and triethylammonium 2-ethoxy-3-dicyanomethylidene-4-oxocyclobut-1-en-1-olate (**4**) in various conditions.

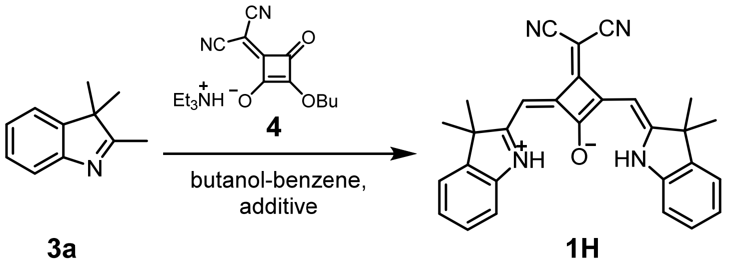

Table S3. Condensation reactions of Fischer's base **2a** with dicyanovinylene-substituted squarate **3**.

entry	temp. /reaction time	butanol/benzene[a]	additive	yield (%)[b]
1	120 °C / 18 h	1:1	non	n. d.
2		1:1	quinoline	n. d.
3		1:1	non	n. d.
4		2:1	*p*-TsOH	2
5		1:1	H_2SO_4	68

[a]Volume ratio. [b]Isolated yield based on **2a**.

6. Crystallization and X-ray structure analysis

Solvent free single crystals of **1H** were obtained by vacuum sublimation, using a thermal gradient sublimation (TGS) system of HTM Reetz GmbH. About 5 mg of raw material were placed into a standard NMR tube as a fine powder. Small pieces of the (100) wafers with a width of 2-3 mm and a length of around 10 mm were placed into an NMR tube (polished side facing up). The NMR tube in turn was positioned between the 1st and 2nd heating zone of the thermal gradient sublimation system. Prior to heating, the system was evacuated for about 2 h until a pressure of at least 2 10^{-6} mbar was reached. Then the 1st and 2nd heating zone were heated up with a rate of ~10 K min^{-1}. The experiment was stopped when single crystals of sufficient size had grown, mainly on the edges of the wafer pieces facing towards the organic material. Single-crystal structure analyses of green needle-like crystals of **1H** having approximate dimensions of 0.087 × 0.081 × 0.033 mm were performed at 100(2) K on a Bruker D8 Quest Kappa diffractometer with a Photon 100 CMOS detector and multilayer monochromatic Cu-K$_\alpha$ radiation. The structure was solved using direct methods, expanded with Fourier techniques and refined with the SHELX software package.[6] All non-hydrogen atoms were refined anisotropically. Hydrogen atoms were included in the structure factor calculation on geometrically idealized positions.

Solvent free single crystals of **1F** were obtained by the slow diffusion of hexane into its chloroform solution. A bronze needle crystal of **1F** having approximate dimensions of 0.750 × 0.200 × 0.150 mm was mounted on a glass fiber. All measurements were made on a Rigaku Mercury70 diffractometer using graphite monochromated Mo-Kα radiation. The structure was solved by a direct methods using the SIR97 program,[7] expanded using the DIRDIF99 program.[8] All the calculations were performed using the CrystalStructure 3.8 software package of the Molecular Structure Corporation.[9]

A summary of the crystallographic data and structure refinement for these two compounds is given in Table S4 Full crystallographic details excluding structure factors have been deposited at the Cambridge Crystallographic Data Centre (CCDC). CCDC-2010755 for **1H** and CCDC-2010897 for **1F** contains the supplementary crystallographic data for this paper. This data can be obtained free of charge from The Cambridge Crystallographic Data Centre via www.ccdc.cam.ac.uk/data_request/cif.

Table S4. Crystallographic data for **1H** and **1F**

	1H	**1F**
Empirical Formula	$C_{29}H_{24}N_4O$	$C_{29}H_{22}F_2N_4O$
Formula Weight	444.52	480.52
T / K	100(2)	293 $\pm$ 1
Color, habit	green, block	bronze, needle
Size, mm	0.087 × 0.081 × 0.033	0.750 × 0.200 × 0.150
Crystal system	Triclinic	triclinic
Lattice Type	Primitive	Primitive
Space group	$P\bar{1}$ (#2)	$P\bar{1}$ (#2)
a / Å	10.6093(9)	10.041(2)
b / Å	11.4966(10)	11.387(2)
c / Å	12.6556(7)	11.654(3)
α / °	63.223(5)	85.675(9)
β / °	69.002(4)	81.578(8)
γ / °	62.815(5)	68.373(6)
V/ Å^3	1203.04(18)	1225.0(4)
Z	2	2
Dcalc / g cm^{-3}	1.227	1.303
F_{000}	468	500.0
μ / cm^{-1}	CuKα, 6.02	MoKα, 0.915
2θmax / °	144.5	61.4
Total reflections	24473	10995
Unique reflections	4734	6456
Reflection/Parameter Ratio	4734/311	11.51
R ($I > 3.00\sigma(I)$^{a}	0.0410	0.0444
Rw ($I > 3.00\sigma(I)$^{b}	0.1120	0.0543
Goodness of Fit Indicator	1.022	1.073

^{a}R = Σ ||Fo| - |Fc|| / Σ |Fo|, ^{b}Rw = [Σ w (|Fo| - |Fc|)^2 / Σ w Fo^2]$^{1/2}$

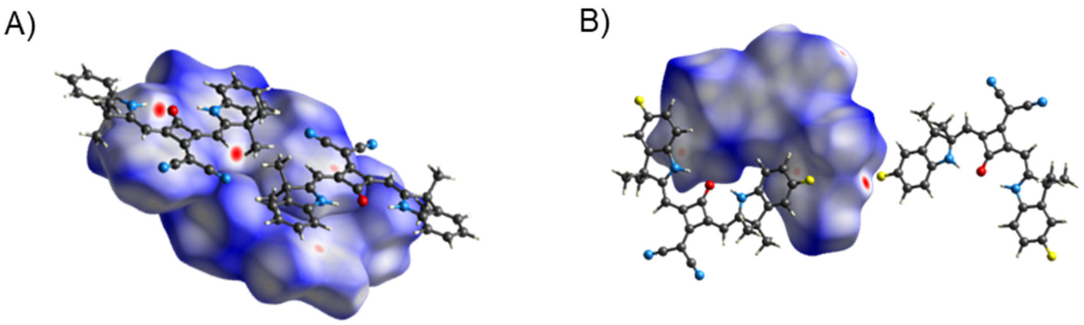

Fig. S3 Hirshfeld isoelectronic surfaces for **1H** (A) and **1F** (D) in single crystals.

Table S5. Transfer integrals calculated from crystal geometries of **1H** and **1F**[a]

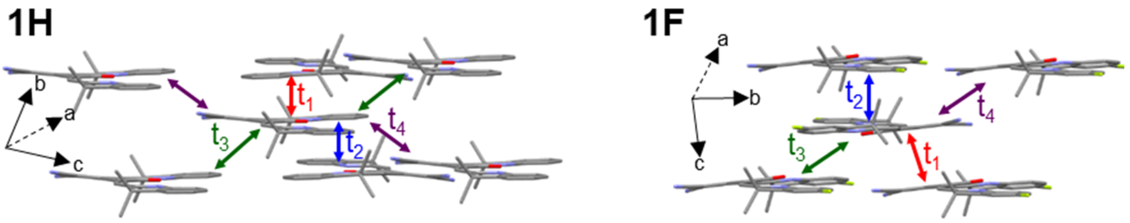

dye	Transfer integral (meV)[b]			
	t_1	t_2	t_3	t_4
1H	−41.5	20.7	13.9	0.115
1F	−13.7	5.38	−4.89	−2.39

[a] Calculated by extended Hückel method [10]. [b] Values of $t_{1\text{-}4}$ correspond to transfer integrals indicated in the figures.

7. Physical properties

Table S6. Electronic absorption, electrochemical, and thermal degradation properties of squaraine dyes.

dye	$\lambda_{\mathrm{max}}{}^{a}$ /nm	ε^{a} /10^{5} $\mathrm{M^{-1}cm^{-1}}$	$\lambda_{\mathrm{onset}}{}^{a}$ /nm	$\lambda_{\mathrm{max,\,film}}{}^{b}$ /nm	$\lambda_{\mathrm{em}}{}^{c}$ /nm	ν_{Stokes} /$\mathrm{cm^{-1}}$	$\Phi_{\mathrm{fl}}{}^{c}$ /%	τ^{c} /ns	$E_{\mathrm{g}}{}^{\mathrm{opt}\,d}$ /eV	$E_{\mathrm{ox}}{}^{e}$ /V	HOMO^{f}	LUMO^{g}	$T_{\mathrm{d5}}{}^{h}$/°C
1H	694	1.26	722	780	712	390	33	2.37	1.72	0.355	−5.51	−3.79	312
1F	697	1.33	726	633	711	280	22	2.24	1.71	0.344	−5.49	−3.78	345
2	683	2.00	710	-	698	340	42	2.24	1.75	0.200	−5.35	−3.60	282

[a] Measured in $CHCl_3$ solutions (5 μM). [b] Measured using 25-nm-thickness films fabricated on a reflective Si/Al/AlOx/TPA substrate. [c] Measured in $CHCl_3$ solutions (1 μM). Lifetimes were determined by fitting the decay curves with a single-exponential decay function [d] Estimated using the onset of the absorption spectrum in solution by $E_{\mathrm{g}}{}^{\mathrm{opt}} = 1240/\lambda_{\mathrm{onset}}$. [e] The oxidation potential was measured on 0.1 M $TBAPF_6$ in CH_2Cl_2 (working electrode: glassy carbon disk; reference electrode: nonaqueous Ag/$AgNO_3$ calibrated with Fc/Fc^{+}; counter electrode: Pt). [f] Estimated from the E_{ox} values assuming a value of −5.15 eV for Fc/Fc^{+}. [g] Calculated from $E_{\mathrm{LUMO}} = E_{\mathrm{HOMO}} - E_{\mathrm{g}}{}^{\mathrm{opt}}$. [h] Temperature corresponding to 5% weight loss obtained from TGA analysis.

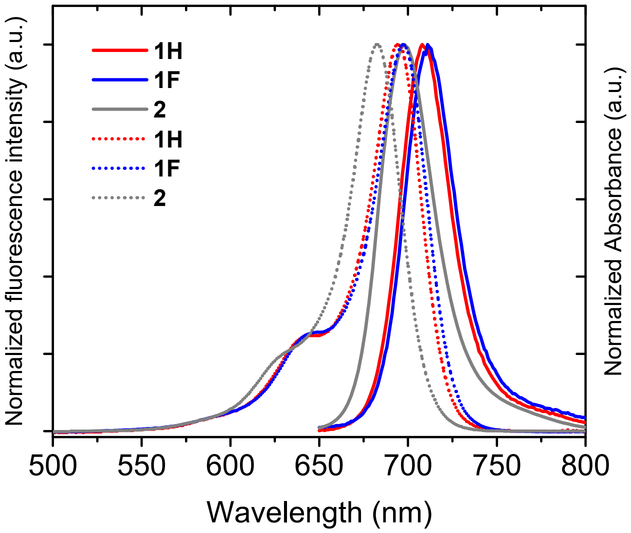

Fig. S4 Absorption ($CHCl_3$, 5 μM, dotted lines) and fluorescence spectra ($CHCl_3$, 1 μM, solid lines) of C_{2v} symmetrical squaraine dyes with intramolecular hydrogen bonding **1H** (red) and **1F** (blue) as well as the *N*-alkylated analogues **2** (gray).

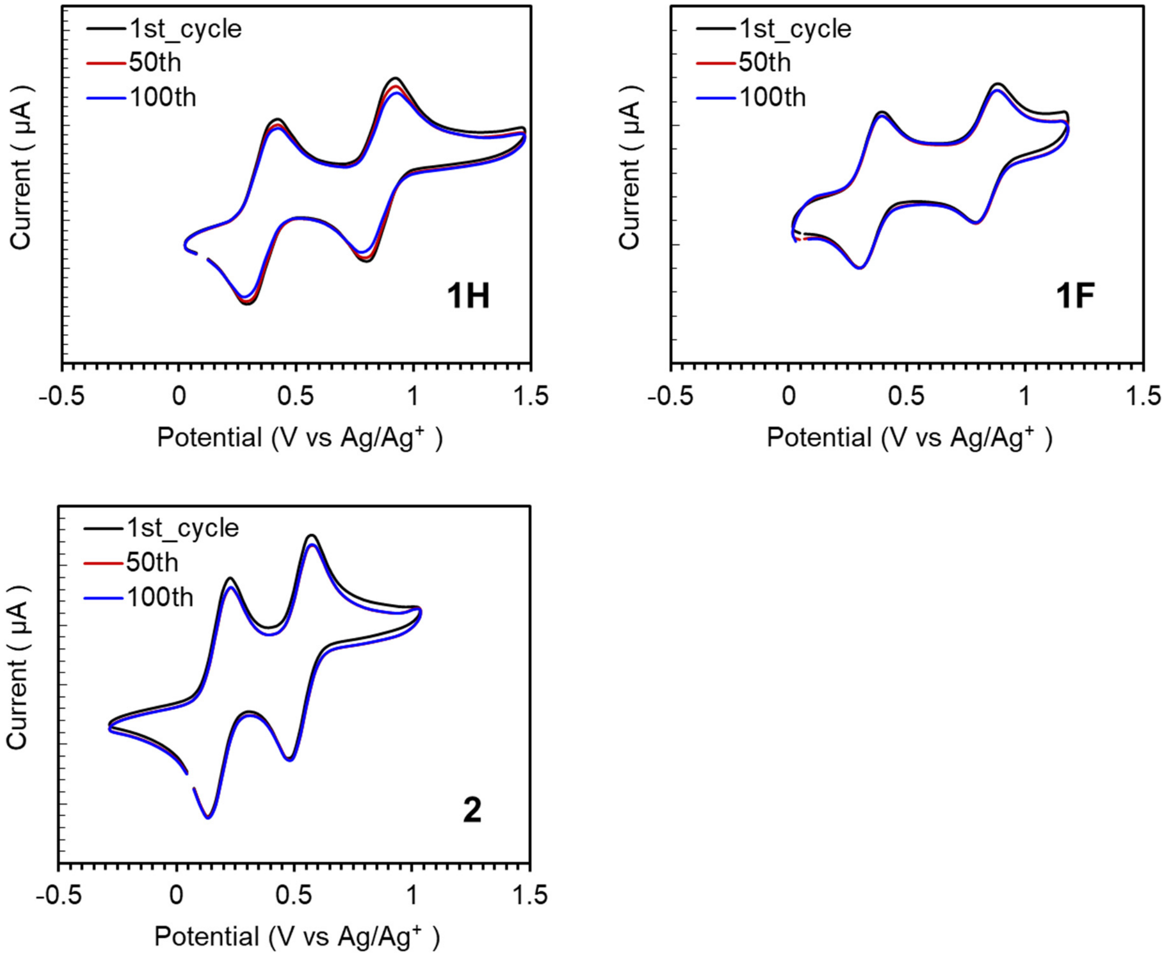

Fig. S5 Multicycle electrochemical stress experiments for **1H** (left top), **1F** (right top), and **2** (left bottom). Cyclic voltammograms of the first (black), the 50th cycle (red), and the 100th scan (blue); 0.1 M tetrabutylammonium hexafluorophosphate was used as a supporting electrolyte. A glassy carbon working electrode, a Pt counter electrode, and a nonaqueous Ag/$AgNO_3$ reference electrode were used; scan rate: 100 mV/s.

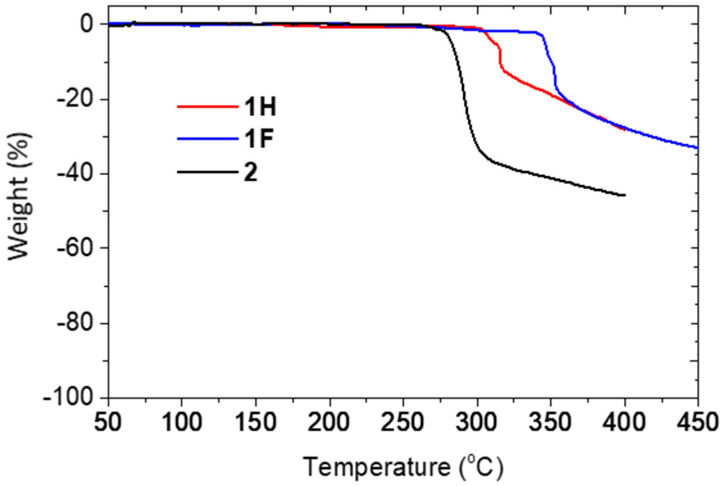

Fig. S6 Thermogravimetric analysis of **1H** (red), **1F** (blue), and **2** (black).

8. OTFT performances

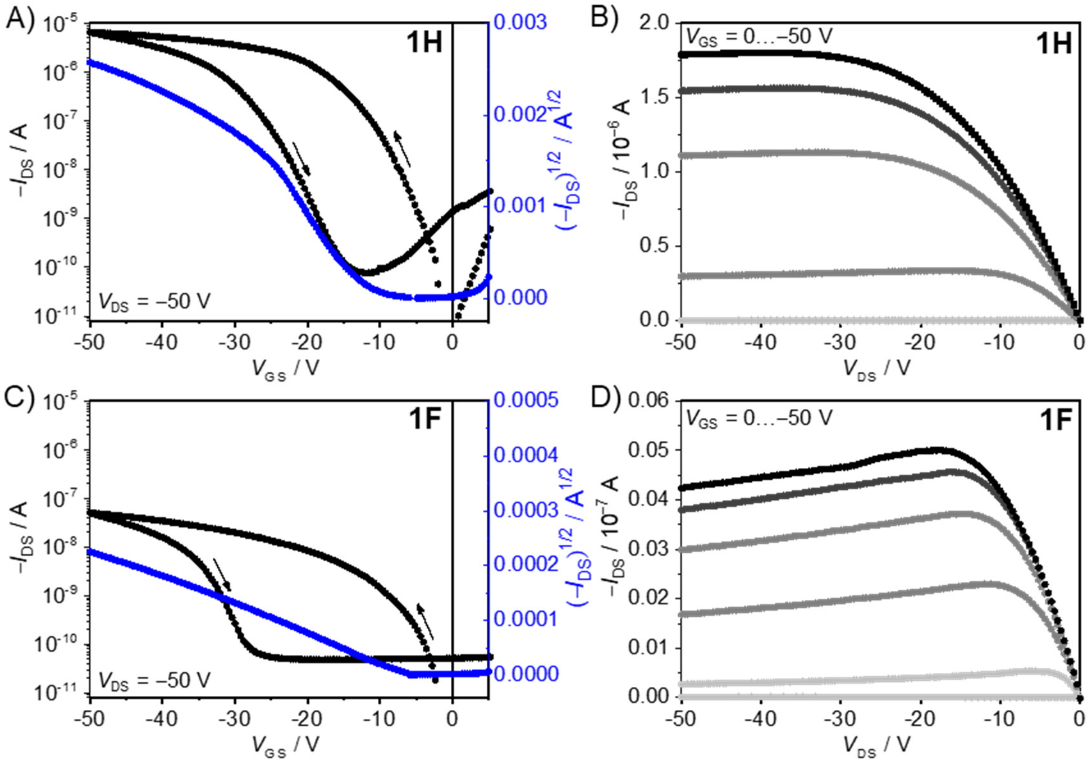

Fig. S7 Transfer and output curves of representative OTFT device with **1H** (A, B) and **1F** (C, D) as organic semiconductor on TPA-modified Si/SiO2/AlOx substrates with gold electrodes.

Table S7. Mobility (μ_h), threshold voltage (V_T) and current on/off ratio (I_{on}/I_{off}) of **1H** and **1F** based transistors on TPA-modified Si/SiO_2/AlO_x substrates with gold electrodes.[a]

dye	T_S / °C	$T_{Sublimation}$ / °C [b]	μ_h / $cm^2 V^{-1} s^{-1}$ [c]	V_T / V [c]	I_{on}/I_{off}
1H	80	158	0.31 ± 0.01	+8	10^6
1F	100	160	$(8.5 \pm 0.3) \times 10^{-4}$	−2	10^4

[a] During the sublimation, the deposition rate was gradually increased up to 0.6 nm min^{-1}, starting with a rate of 0.2 nm min^{-1} at the sublimation temperature $T_{Sublimation}$ for the first 10 nm of the thin film. The substrates were heated to the given substrate temperature T_S; [b] Sublimation temperature $T_{Sublimation}$ corresponding to a deposition rate of 0.2 nm min^{-1}; [c] Average value of at least ten transistor devices.

9. NMR and MS spectra

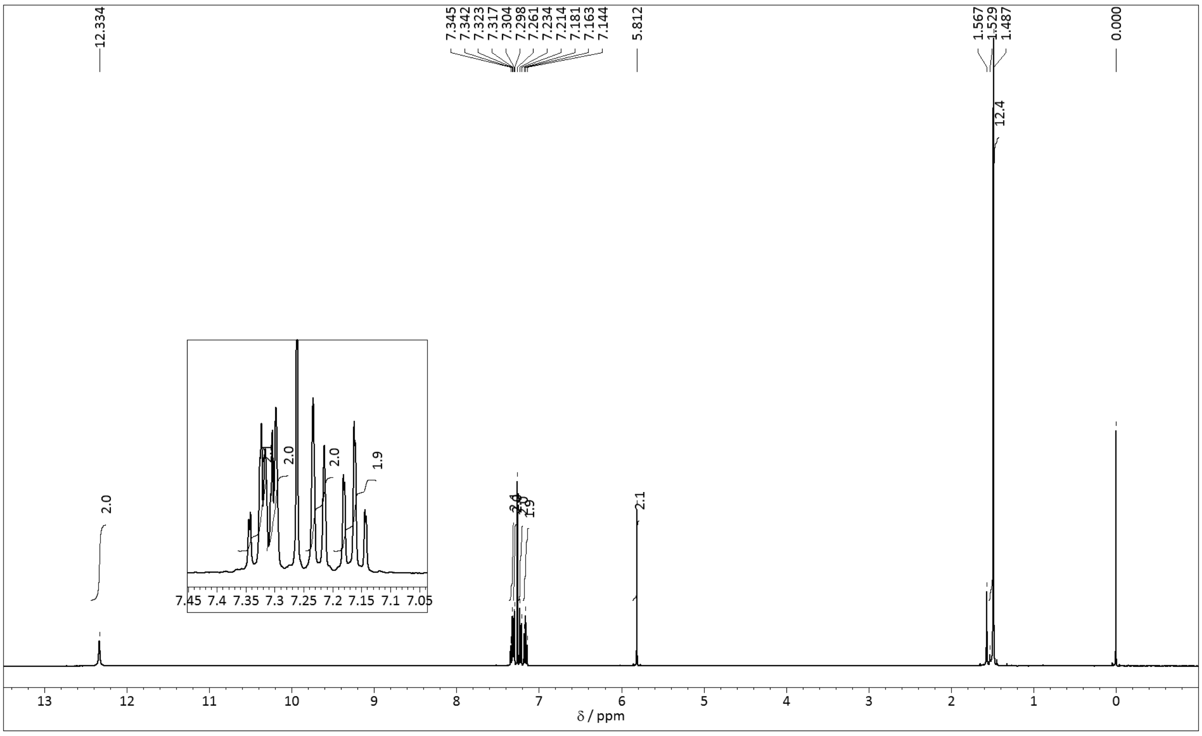

Fig. S8 ^{1}H-NMR spectrum ($CDCl_3$, 25 °C) of **1H**.

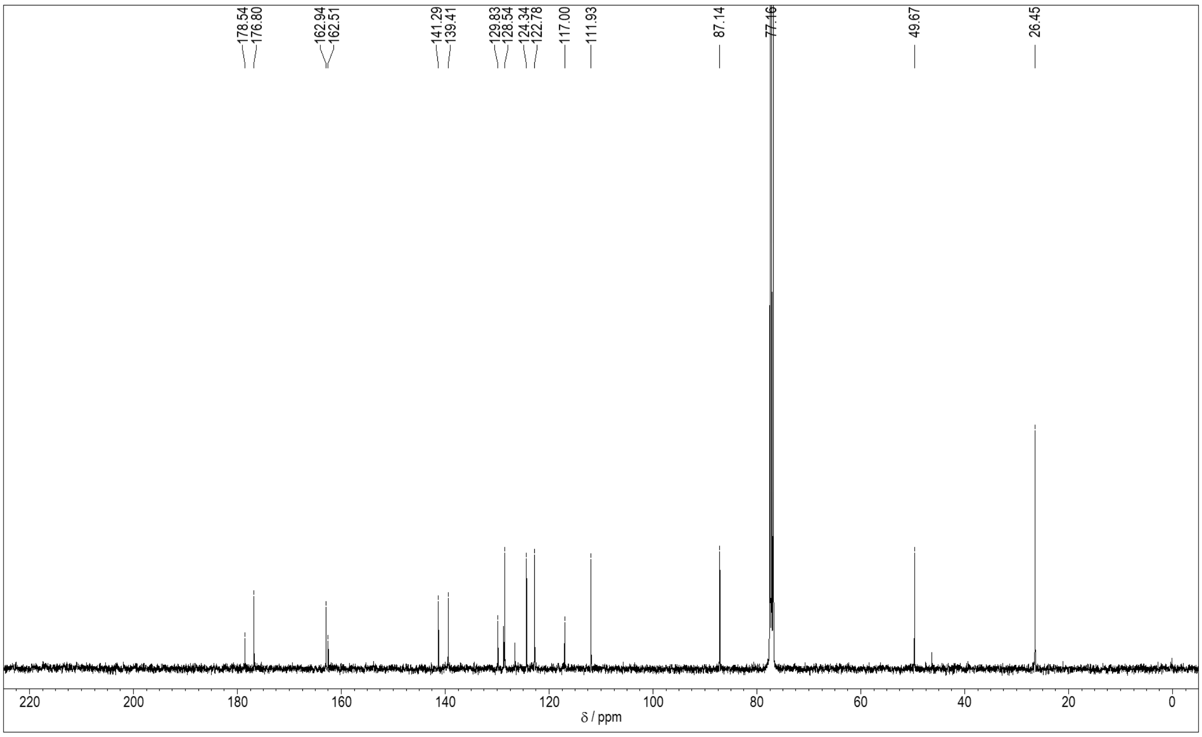

Fig. S9 ^{13}C-NMR spectrum ($CDCl_3$, 25 °C) of **1H**.

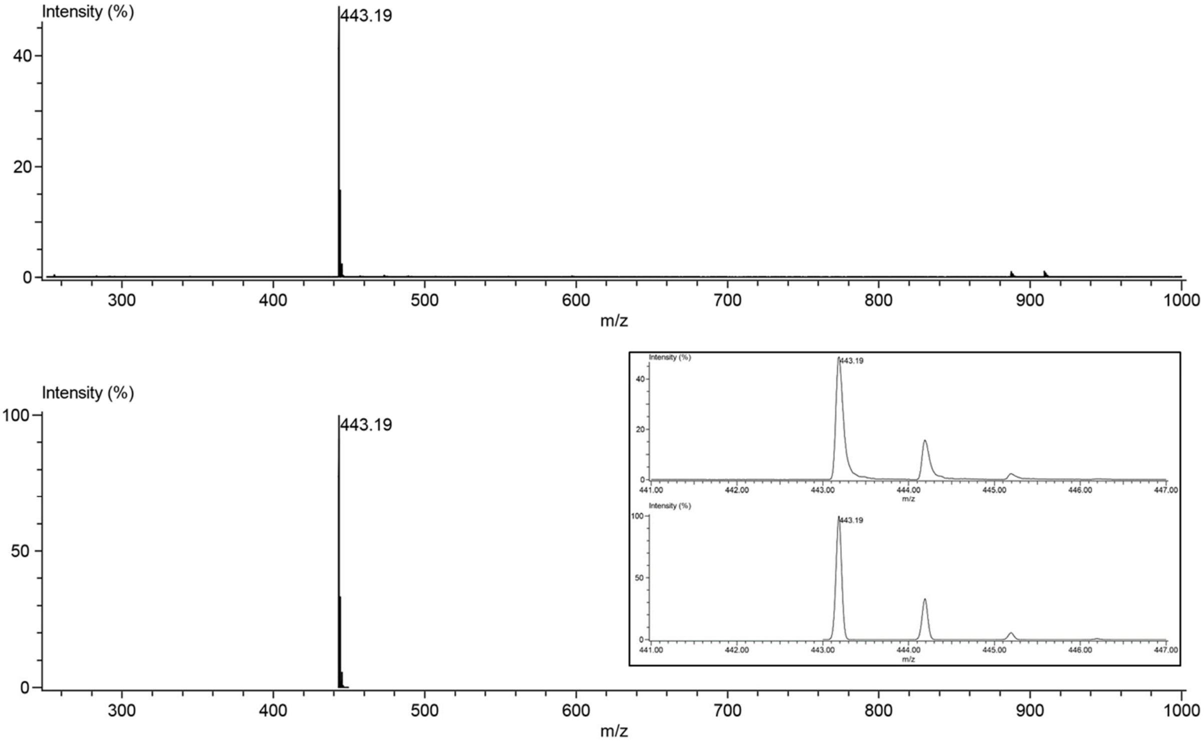

Fig. S10 ESI-MS spectrum of **1H**.

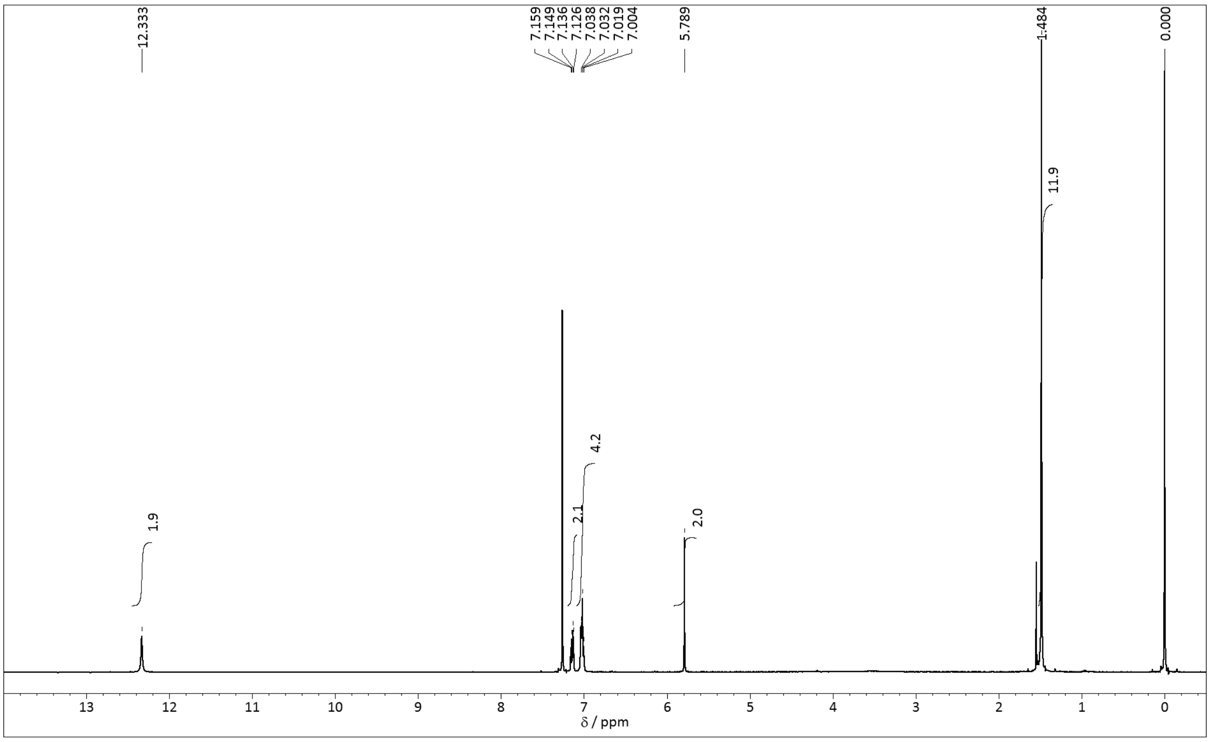

Fig. S11 ^{1}H-NMR spectrum ($CDCl_3$, 25 °C) of **1F**.

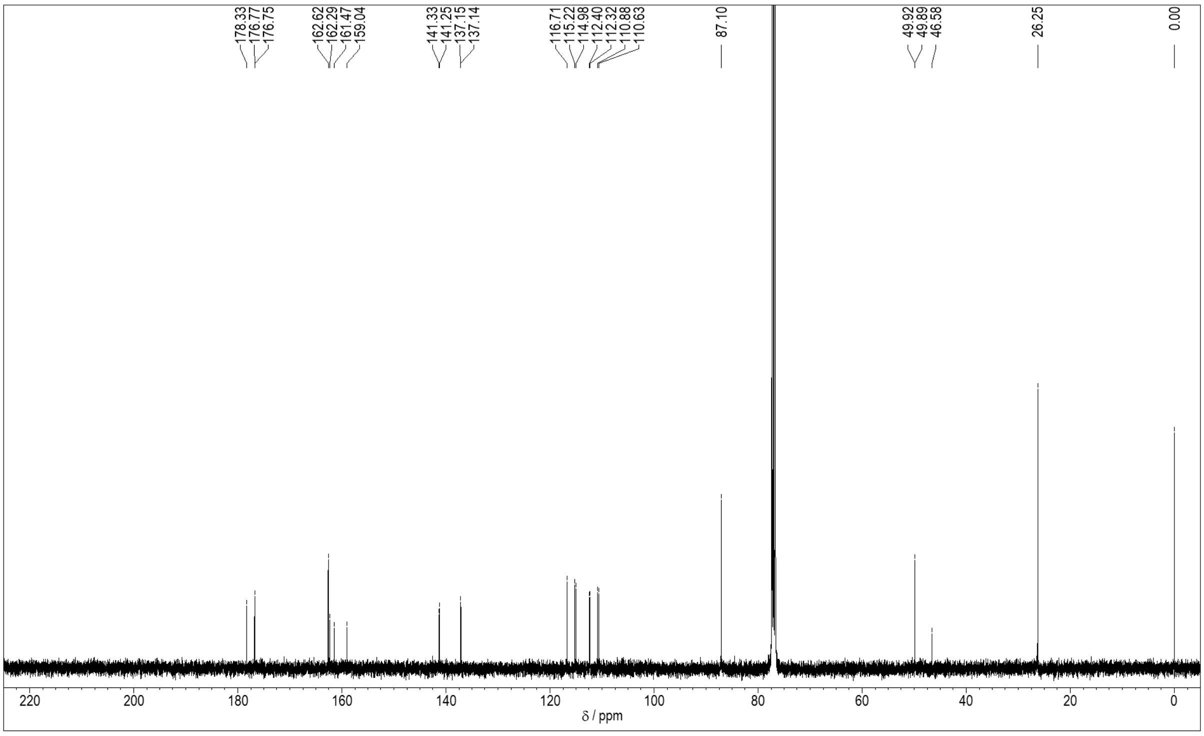

Fig. S12 ^{13}C-NMR spectrum (CDCl$_3$, 25 °C) of **1F**.

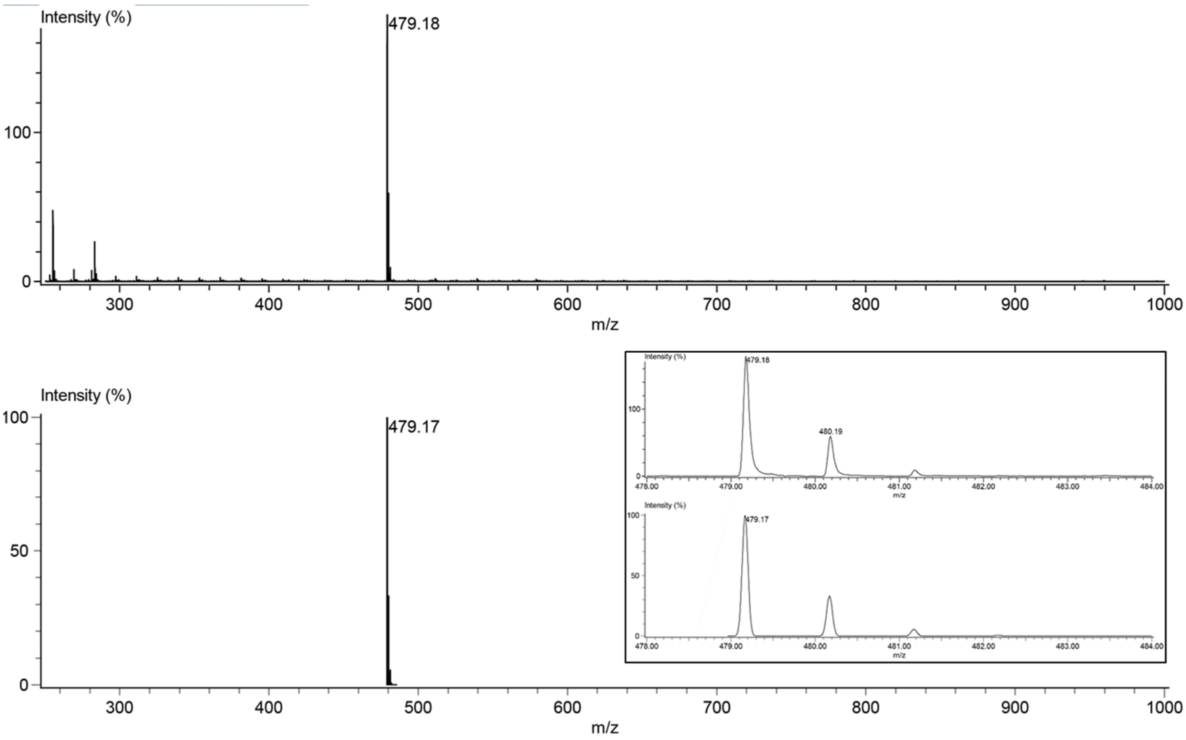

Fig. S13 ESI-MS spectrum of **1F**.

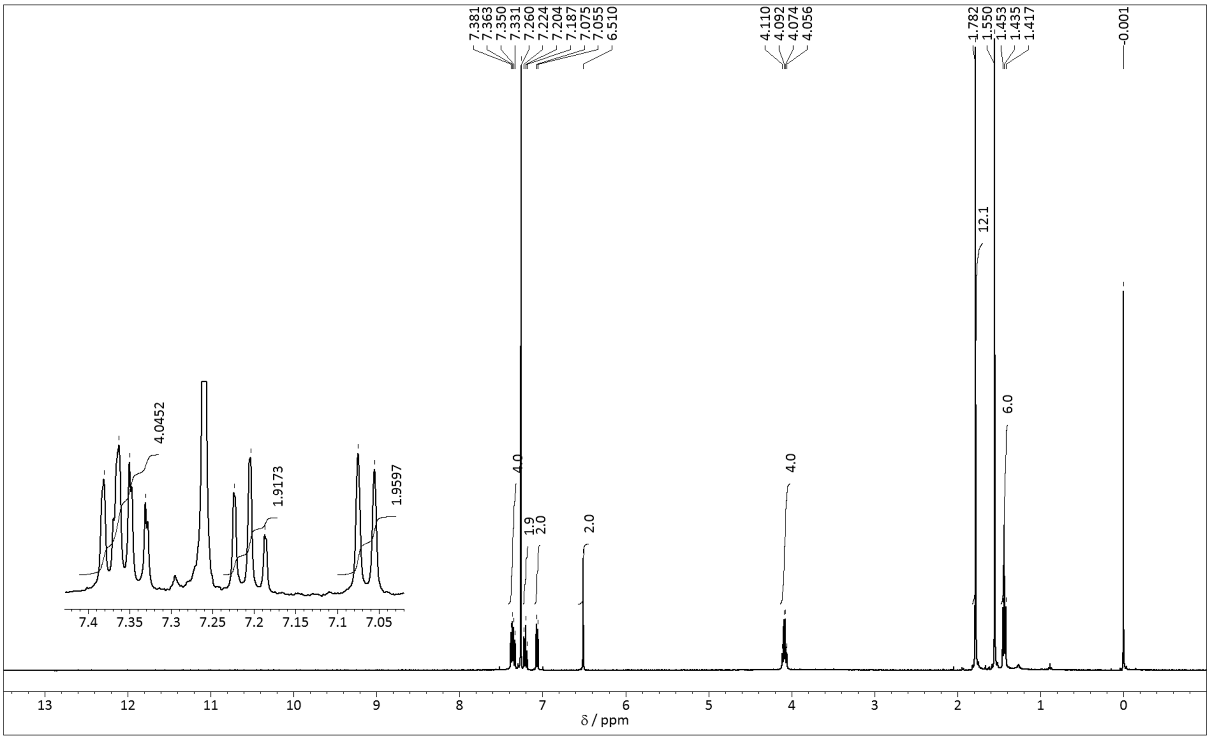

Fig. S14 ^{1}H-NMR spectrum (CDCl₃, 25 °C) of **2**.

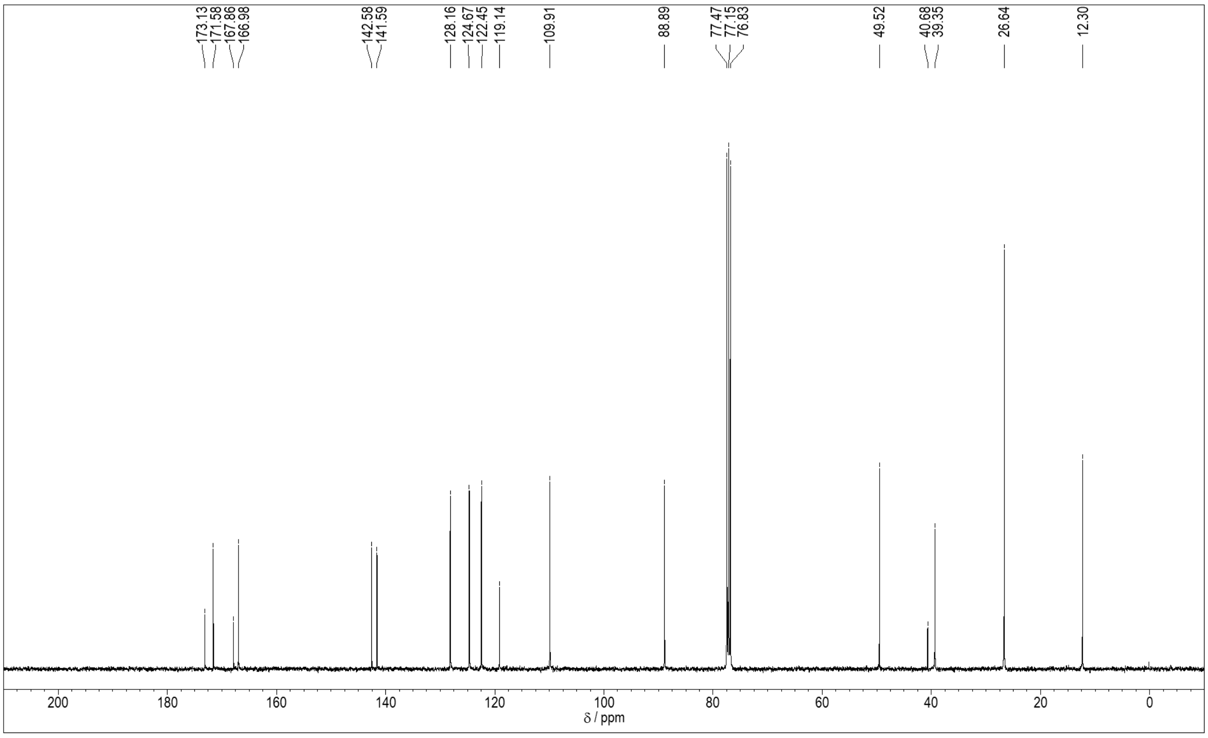

Fig. S15 ^{13}C-NMR spectrum (CDCl₃, 25 °C) of **2**.

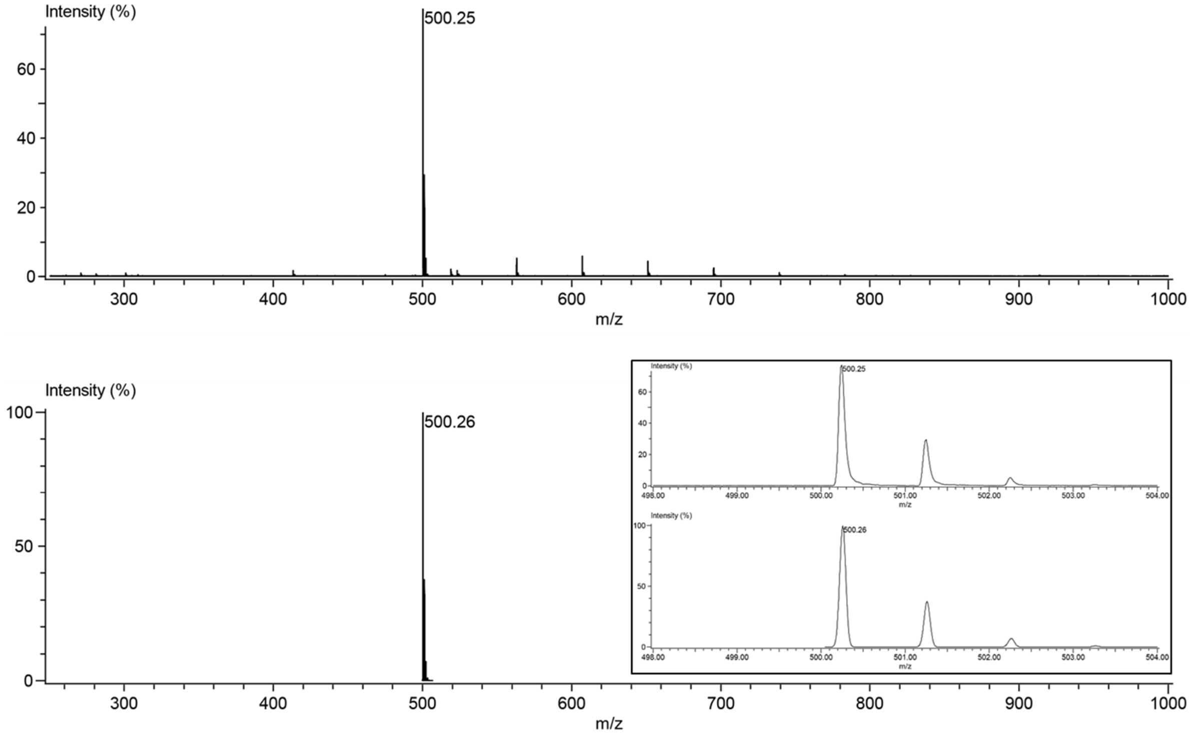

Fig. S16 ESI-MS spectrum of **2**.

10. References

1. Jiao, L. Y.; Oestreich, M. *Chem. Eur. J.*, **2013**, *19*, 10845.
2. Mayerhöffer, U.; Gsänger, M.; Stolte, M.; Fimmel, B.; Würthner, F. *Chem. Eur. J.*, **2013**, *19*, 218.
3. Zubatyuk, R. I.; Baumer, V. N.; Tatarets, A. L.; Patsenker, L. D.; Shishkin, O. V. *Acta Crystallogr. Sect. E Struct. Reports Online*, **2004**, *60*, 2252.
4. Gaussian 09, Revision **A.1**, Frisch, M. J.; Trucks, G. W.; Schlegel, H. B.; Scuseria, G. E.; Robb, M. A.; Cheeseman, J. R.; Scalmani, G.; Barone, V.; Mennucci, B.; Petersson, G. A.; Nakatsuji, H.; Caricato, M.; Li, X.; Hratchian, H. P.; Izmaylov, A. F.; Bloino, J.; Zheng, G.; Sonnenberg, J. L.; Hada, M.; Ehara, M.; Toyota, K.; Fukuda, R.; Hasegawa, J.; Ishida, M.; Nakajima, T.; Honda, Y.; Kitao, O.; Nakai, H.; Vreven, T.; Montgomery, Jr., J. A.; Peralta, J. E.; Ogliaro, F.; Bearpark, M.; Heyd, J. J.; Brothers, E.; Kudin, K. N.; Staroverov, V. N.; Kobayashi, R.; Normand, J.; Raghavachari, K.; Rendell, A.; Burant, J. C.; Iyengar, S. S.; Tomasi, J.; Cossi, M.; Rega, N.; Millam, N. J.; Klene, M.; Knox, J. E.; Cross, J. B.; Bakken, V.; Adamo, C.; Jaramillo, J.; Gomperts, R.; Stratmann, R. E.; Yazyev, O.; Austin, A. J.; Cammi, R.; Pomelli, C.; Ochterski, J. W.; Martin, R. L.; Morokuma, K.; Zakrzewski, V. G.; Voth, G. A.; Salvador, P.; Dannenberg, J. J.; Dapprich, S.; Daniels, A. D.; Farkas, Ö.; Foresman, J. B.; Ortiz, J. V.; Cioslowski, J.; Fox, D. J. Gaussian, Inc., Wallingford CT, 2009.
5. Law, K.-Y.; Bailey, F. C. *Can. J. Chem.,* **1986**, *64*, 2267–2273.
6. Sheldrick, G. A short history of SHELX Acta Cryst. A 2008, 64, 112-122.
7. Altomare, A.; Burla, M. C.; Camalli, M.; Cascarano, G. L.; Giacovazzo, C.; Guagliardi, A.; Moliterni, A. G. G.; Polidori, G.; Spagna, R. J. Appl. Cryst. **1999**, *32*, 115-119.
8. Beurskens, P. T.; Admiraal, G.; Beurskens, G.; Bosman, W. P.; Garcia-Granda, S.; Gould, R. O.; Smits, J. M. M.; Smykalla C. The DIRDIF99 program system, Technical Report of the Crystallography Laboratory at University of Nijmegen; University of Nijmegen: Nijmegen, The Netherlands, 1999.
9. CrystalStructure 3.8: Crystal Structure Analysis Package, Rigaku and Rigaku Americas (2000-2007). 9009 New Trails Dr. The Woodlands TX 77381, U.S.A.
10. Mori, T.; Kobayashi, A.; Sasaki, Y.; Kobayashi, H.; Saito, G.; Inokuchi, H. *Bull. Chem. Soc. Jpn.*, **1984**, *57*, 627–633.